J Phys. A: Math. Gen. 24 (1991) 2793–2805 Printed in the UK

Dimension and escape rate of chaotic scattering from classical and semiclassical cross section data

Christof Jung† and Tamás Tél‡

Institut für Festlörperforschung, Forschungszentrum Julich, D-5170 Jülich, Federal Republic of Germany

Received 29 January 1991

Abstract. A new method is presented to extract information concerning the strange repeller underlying chaotic potential scattering based on classical and quantum mechanical scattering cross section data in the semiclassical limit. In particular, we show that both the fractal dimension and the escape rate of the classical system can be deduced from quantum measurements. The method can be applied in the limit of small $\hbar$ or small wavelength of the incoming projectile compared with the size of the target. As input, the differential quantum cross section is needed against the angle and/or the energy in such a good resolution that fast interference oscillations are well resolved.

1. Introduction

Even though the phenomenon of chaotic scattering has been known in numerical model computations for 20 years (for review see [1–3]), the investigation of deeper problems has only recently been started, and some interesting aspects of experimental importance are still open. The most spectacular feature of classical scattering chaos is a complicated deflection function having singularities on a *fractal* set (a manifestation of the 'sensitivity to initial conditions'). This behaviour is due to the existence of a *chaotic repeller* [4] in phase space. Its topological structure and quantitative connection to the singularities of the deflection function have been investigated in several case studies [5–16] of potential scattering. The knowledge of the deflection function provides us with information on the structure of the repeller and, in particular, on the most important quantitative characteristics like (partial) fractal dimension D_0, escape rate κ and Lyapunov exponent λ.

Unfortunately, the deflection function is hard to obtain even in classical experiments and is not at all measurable in micro-systems. Its measurement would require an exact preparation of momentum and impact parameter of the projectile. However, these two quantities are conjugate, and according to quantum mechanical uncertainty, they cannot be specified simultaneously with unlimited accuracy. In usual scattering experiments the momentum is specified as precisely as possible, and the impact parameter is completely unspecified. The quantity which is really measured both classically and quantum mechanically is the *differential cross section* as a function of angle and/or energy. The maximal information which can be obtained from a scattering experiment on micro-systems is provided by the differential cross section.

† On leave of absence from Fachbereich Physik, Universität Bremen, FRG.
‡ On leave of absence from Institute for Theoretical Physics, Eötvös University, Budapest, Hungary.

0305-4470/91/122793+13$03.50

It is of particular interest if one can decide from quantum cross section data whether the classical scattering is chaotic and if one can extract D_0, κ and λ out of these data. Of course, an affirmative answer is expected to exist in the semiclassical limit only. One possible way is a statistical analysis of the fluctuations in the cross section: a computation of the correlations and a check for properties which we expect for random matrix theory. This procedure was shown to yield the escape rate and has been applied to several examples [2, 17]. In the present paper we introduce another method from which not only the escape rate κ but also the fractal dimension D_0 can be deduced. From these two data the Lyapunov exponent λ can be estimated.

In section 2 we first extract D_0 out of the classical cross section by investigating the pattern of rainbow singularities in two degrees of freedom systems. One might hope that a similar method also works for the quantum mechanical cross section. Unfortunately, this is not the case and we shall see in more detail why not. The quantum cross section, however, has an important type of structure that the classical cross section does not have, namely interference oscillations. In section 3 we use these oscillations appearing already in the semiclassical approximation to extract D_0 and κ by means of a new type of scaling argument. The technical details of the method are relegated to an appendix.

As an illustrative example we take a scattering system for which the repeller is completely known [5, 14]. The process is defined by the following two variable potential

$$V(x,y)=e^{-(x+\sqrt{2})^2-y^2}+e^{-(x-1/\sqrt{2})^2-(y+\sqrt{3/2})^2}+e^{-(x-1/\sqrt{2})^2-(y-\sqrt{3/2})^2}. \qquad (1)$$

To the best of our knowledge n-hill problems, a special case of which is provided by (1) for $n=3$, are the only scattering processes known so far with the following properties: (i) the potential decreases sufficiently fast in all directions so that the asymptotic conditions of scattering theory are fulfilled, (ii) the potential is smooth, (iii) the symbolic dynamics of the repeller is known in a globally exact form and turns out to be complete.

Property (iii) is irrelevant from the point of view of our analysis. It only makes easier the investigation of the classical repeller and the determination of quantities like D_0, κ, λ. In section 2 we work with classical rainbow singularities. Therefore, we need a smooth potential where the rainbows have generic structure. Billiard scattering systems with hard wall targets, which are the subject of quite extensive investigation [6, 7, 9, 11, 13, 15], do not show generic rainbows and are thus not suitable for demonstrating the arguments of section 2. The general results of the semiclassical analysis, however, do not rely upon smoothness properties and are valid for all cases fulfilling property (i).

2. The pattern of rainbow singularities

As has been explained in [18], the most spectacular feature of chaos manifested in the classical differential cross section as a function of the angle is an infinity of rainbow singularities. They are arranged in a fractal pattern reflecting the structure of the underlying chaotic repeller in phase space.

Let us give a short outline of the explanation: in a measurement of the cross section the incoming momentum p_{in} is fixed and the impact parameter axis is covered evenly by incoming particles. In the case of chaotic scattering, the impact parameter line splits into an infinity of intervals I_j in which the deflection function $\theta(b)$ is continuous, and

the boundaries of the I_j are points of discontinuity. Here θ is the scattering angle and b is the coordinate along the impact parameter line. Let us assume that the set $\{I_j\}$ of intervals is ordered according to their lengths r_j: $j>j'$ if $r_j<r_{j'}$. In each interval I_j the deflection function oscillates smoothly and creates a rainbow singularity in the cross section at each of its relative *extrema*. Trajectories starting in shorter intervals I_j stay longer near the repeller and leave its neighbourhood closer to some branch of its *unstable manifold*. The intersection of these branches with a plane reflects the fractal structure of the repeller itself. We can represent such a cut in angular momentum and angle variables and consider its projection on to the angle axis. Accordingly, the angular minima and maxima of the manifold are also arranged in this fractal pattern. The minima and maxima of the deflection function (i.e. the rainbows) accumulate towards these angular extrema of the manifold. Thus, the distribution of the rainbows along the angle axis reflects the fractal pattern of the chaotic set in phase space. In particular, the fractal dimension of the rainbow-pattern is expected to coincide with the partial fractal dimension D_0 [4] of the repeller. (The total dimension in a three variable autonomous flow can be expressed as $2D_0+1$.) Thus, measuring the dimension of the set where the rainbow singularities sit should yield D_0. A non-zero value of the partial *fractal dimension is a sign of chaotic scattering.*

There is, however, a practical difficulty which makes the determination of D_0 non-trivial. This is due to the huge number of very weak rainbow-singularities which cannot be distinguished from a smooth background. With unlimited accuracy, one could see an infinity of rainbow singularities. They all are locally described by a function of type $A_j|\theta-\theta_{Rj}|^{-1/2}$ on one side of the rainbow position θ_{Rj}, and by a constant on the other side. This follows from the fact that

$$c=\left|\frac{\mathrm{d}\theta}{\mathrm{d}b}(b)\right|^{-1} \tag{2}$$

is the contribution of a trajectory with impact parameter b to the differential cross section. Close to a local extremum θ_{Rj} of the deflection function, we can write $\theta(b)=\theta_{Rj}-a(b-b_j)^2$ from which $c\sim|(b_i-b_j)|\sim|\theta-\theta_{R,j}|^{1/2}$ is obtained. The peaks are sharp and, therefore, θ_{Rj} can, in principle, be determined exactly from the cross section. By using a finite resolution, i.e. by dividing the angle variable in a finite number of boxes, the height of a peak in a box is given by

$$w_j=\int A_j|\theta-\theta_{Rj}|^{-1/2}\,\mathrm{d}\theta$$

where the integration runs from θ_{Rj} to the boundary of the box in which θ_{Rj} lies. Unfortunately, the weights A_j and, therefore, also the weights w_j decrease *exponentially* rapidly for increasing j [18]. In addition, the very weak rainbows are grouped together very densely on the θ axis, so that they cannot be resolved. Consequently, we only can read off a finite number of strongest rainbows. The rest are not separated, or disappear in the statistical fluctuations. Thus, we expect to be able to identify only a few (of order 100) singularities, and the task is to try to get the number D_0 out of these data.

For this purpose, we recommend to use a method that has been shown to be much more efficient than box counting, in connection with both dynamical systems [19] and growth processes [20]. The idea is to distribute points *uniformly* on the fractal and use these as centres of balls of radius R. Then count the number of points $N(R)$ of the

fractal falling in such a box. The average of $1/N(R)$ over all balls should scale with the radius as R^{-D_0} [19, 20], i.e.

$$\langle N^{-1}(R)\rangle \sim R^{-D_0}$$

where D_0 is the fractal's dimension. If only a few (n) points of the fractal are known, we can take all of them as centres, count the numbers $N_i(R)$ of points falling in ball i, and use the formula

$$-\ln\left(\frac{1}{n}\sum_{i=1}^{n} N_i^{-1}(R)\right) = D_0 \ln R + \text{constant} \tag{3}$$

to estimate the fractal dimension. R can change between the lower cutoff δ of the system (the degree of resolution) and the total linear size L. Relation (3) is expected to hold for $R \ll L$. If the number of fractal points is low, the system seems to be a set of isolated points on very fine scales. Thus, the true fractal behaviour can show up only in an intermediate range $\delta \ll R \ll L$.

Let us apply now this method to a numerical example. We take system (1) with an incoming momentum $p_{in} = (-1.0, 0.0)$. This corresponds to an energy $E = 0.5$ of the projectile, being quite close to the saddle energy of the potential $E_s \approx 0.458$. For $E = 0.5$ we obtained the partial fractal dimension of the repeller, from the discontinuities of the deflection function, as $D_0 = 0.59$ which is not too small. (With increasing energy, D_0 would decrease rapidly and would go to zero at the hill maximum $E_m \approx 1.005$ of potential (1) [12].)

The impact parameter interval $I_c = [0.08, 0.28]$ has been covered evenly with 10^6 incoming particles. Initial conditions outside I_c do not contribute to rainbows, they only give a smooth background in the cross section which is irrelevant for our considerations. Further, we have divided the angle interval between 46 and 74 degrees (a range where the unstable manifold of the repeller extends to infinity) into 28 000 boxes of length 10^{-3} degrees and counted how often they were hit by outgoing particles. The result is plotted in figure 1. It gives the differential cross section without the smooth background coming from b values outside I_c. At this resolution we could identify only 66 rainbow singularities clearly.

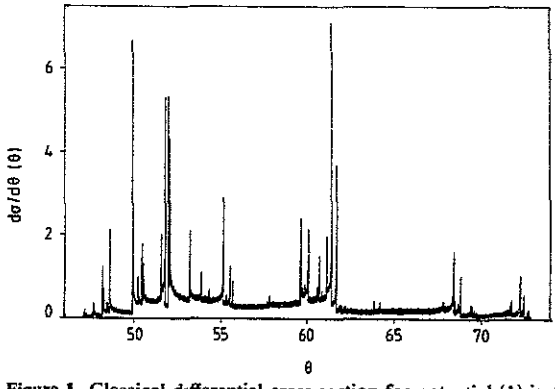

Figure 1. Classical differential cross section for potential (1) in the angular interval [46°, 74°] taken at $E = 0.5$, $\alpha = \pi$

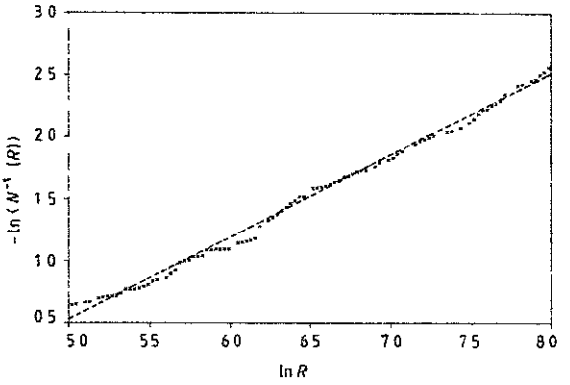

Figure 2. Computation of the fractal dimension for the 66 singularities identified in figure 1, based on the method described by (3) The dashed line has a slope of 0.66

Measuring the number of points $N_i(R)$ falling in ball i ($i = 1, 66$) we did find a linear behaviour (3) over two decades of R as illustrated in figure 2 (although no straight line can be seen on the usual $\ln N$ against $\ln 1/\varepsilon$ plot of the box counting method). As a result we obtain $D_0 \approx 0.66$ which has to be compared with the exact result $D_0 = 0.59$. It is easy to understand why this value is somewhat too large: since densely clustered weak rainbows are not resolved, we only see the strong ones which are more evenly distributed than the totality of all rainbows.

Finally, we ask what would happen if we tried to apply the same method to quantum mechanical data? In the quantum cross section the rainbows are not completely sharp; they acquire a width proportional to $\hbar^{2/3}$. In addition, the shape of the peaks is strongly influenced by interferences, so that it is extremely difficult to locate the actual rainbow angles with sufficient accuracy even at small values of $\hbar$. (What the rainbows look like in a semiclassical calculation for our model system (1) has been shown in [21].) Therefore, the method to determine D_0 from the rainbows of the quantum differential cross section seems to be hopeless. In the next section we work out a completely different approach based on the properties of interference oscillations.

3. The pattern of interference oscillations

When comparing classical and the quantum differential cross sections of the same system, the most spectacular differences are the quantum mechanical interference oscillations. In this section we demonstrate that on a semiclassical level they contain relevant information concerning the classical repeller.

In a semiclassical approximation the scattering amplitude is given by [22]:

$$f(\alpha, E, \theta) = \sum_j \sqrt{c_j} \exp(\mathrm{i}S_j/\hbar - \mathrm{i}\pi\mu_j/2) \tag{4}$$

provided the angle θ is *away* from the classical rainbow singularities: $\theta \neq \theta_{Rj}$. The sum runs over all classical scattering trajectories Γ_j coming in with a specified incoming direction α and energy E and going out with the measured scattering angle θ. c_j is the contribution of trajectory Γ_j with impact parameter b_j to the classical differential cross section and is given by (2) taken at $b = b_j$. The quantity $S_j = -\int_{\Gamma_j} q\,\mathrm{d}p$ is the

reduced action [22] of trajectory Γ_j, and μ_j is its Maslov index, i.e the number of caustics met by the trajectory. The differential cross section is then obtained as

$$\frac{d\sigma}{d\theta}(\alpha, E, \theta) = |f(\alpha, E, \theta)|^2. \tag{5}$$

Let us investigate the interference effects in (5) in the limit of small $\hbar$. In principle, c_j is a slowly varying function of α, E and θ. Investigating very small intervals of E and θ only, the variation of c_j is irrelevant, and in our present derivation we can take the function c_j at some reference value α_0, E_0, θ_0. Let us stay away from caustics, so that the number of contributions to (4) does not change and μ_j stays constant. The only source of rapid variation is then the phase $S_j/\hbar$ because the classical action is divided by a small quantity $\hbar$.

First, we keep $E = E_0$ fixed and expand S_j linearly around θ_0:

$$S_j(\theta) = S_j(\theta_0) + (\theta - \theta_0)L_j \tag{6}$$

where $L_j = \partial S_j/\partial\theta(\theta_0)$ is the outgoing angular momentum of trajectory Γ_j. The cross section then becomes

$$\frac{d\sigma}{d\theta}(\alpha_0, E_0, \theta) = \sum_j c_j + \sum_{k<j} 2\sqrt{c_k c_j}\cos(\varphi_{kj} - \theta(L_k - L_j)/\hbar) \tag{7}$$

where the φ_{kj}s are constant. The first term is the classical contribution; the double sum represents the interference oscillations. As has been explained in [21, 23], the values of angular momentum differences define a fractal set reflecting the fractal pattern of the chaotic repeller. Based on this idea, let us take at fixed α_0, E_0 the Fourier transform

$$g(L) \equiv \int \frac{d\sigma}{d\theta}(\theta)\cos\left(\frac{\theta L}{\hbar}\right) d\left(\frac{\theta}{\hbar}\right) \tag{8}$$

of the differential cross section over a suitable range of θ around some θ_0 away from classical rainbow positions. One can then analyse the positions of the frequency contributions and determine their fractal dimension. Unfortunately, with this direct method we did not succeed in numerical examples due to the rather uneven resolution of $g(L)$ (see figure 3). We had better success with the following strategy.

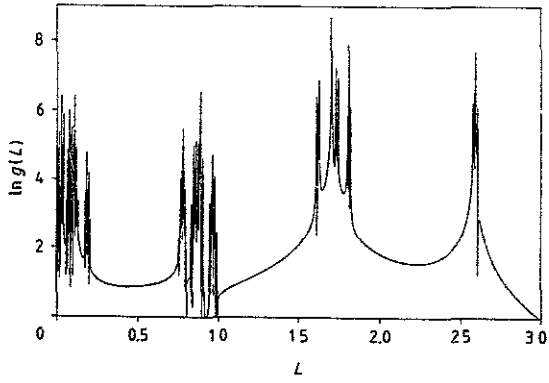

Figure 3. Logarithm of $g(L)$, of the Fourier transform of the semiclassical differential cross section (computed in [21]) as a function of angle for $E = 0.6$, $\alpha = \pi$

Consider the plot of $g(L)$, where the frequency (angular momentum difference) axis has been divided into identical boxes. Take a variable threshold S and count the number $Z(S)$ of boxes whose content is larger than S. The exact $Z(S)$ is a step function In the following, however, we consider a smooth approximation to it. We claim that this function exhibits the scaling behaviour

$$Z(S) \sim \left(\frac{S_M}{S}\right)^{2D_0} \ln\left(\frac{S_M}{S}\right). \tag{9}$$

Here S_M is the largest box content, and D_0 is the partial fractal dimension of the repeller. A derivation of (9) is given in the appendix.

Taking the logarithm of (9) yields

$$\ln Z(S) = 2D_0 \ln\left(\frac{S_M}{S}\right) + \ln\left(\ln\left(\frac{S_M}{S}\right)\right) + \text{constant}. \tag{10}$$

This relation provides a simple method for obtaining the fractal dimension D_0: measure $Z(S)$ and S_M, and consider the plot $\ln Z(S) - \ln(\ln(S_M/S))$ against $\ln(S_M/S)$. In the range $S < S_m$ a straight line should be found with slope $2D_0$.

Let us apply this method to our illustrative example (1). We took $\hbar = 2\times 10^{-7}$, $\alpha_0 = \pi$, picked out the θ interval [5.4, 5.402], and computed the cross section with a semiclassical method described in [21]. For such a small value of $\hbar$ a numerical solution of the Schrödinger equation would be hopeless-but the semiclassical approximation is expected to be excellent. The energy is chosen to be $E_0 = 0.6$, because at this value the semiclassical sum (4) is already sufficiently rapidly absolutely converging. (At $E = 0.5$, which we have taken in section 2 for the classical cross section, the semiclassical sum is only oscillatory convergent.) The Fourier transform $g(L)$ of this cross section is shown in figure 3. Here the frequency axis has been divided into 8192 boxes. A comparison of this plot with that of the classical angular momentum differences shown in figure 2 of [23] shows that $g(L)$ is really a broadened version of the classical distribution.

After determining the function $Z(S)$ from figure 3, we obtain the plots of figure 4. The graph of figure 4(a) seems to have a constant curvature but on the plot where the logarithmic correction has been subtracted (figure 4(b)) we find an approximately

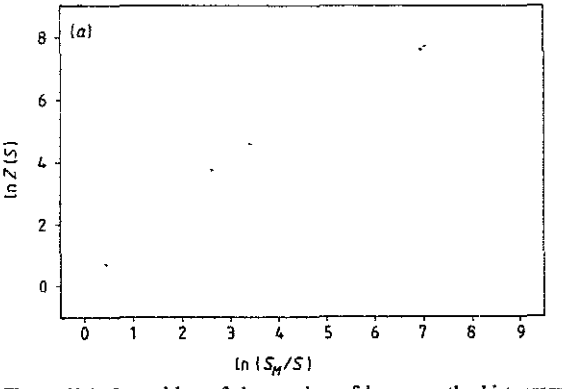

Figure 4(a). Logarithm of the number of boxes in the histogram of $g(L)$ with contents larger than S against the logarithm of S_M/S ($S_M = 5900$)

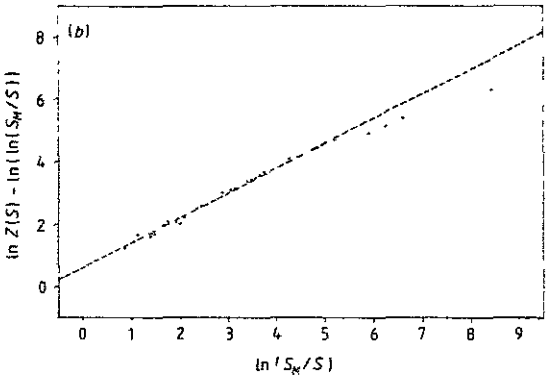

Figure 4(*b*). As figure 4(*a*), but with the logarithmic correction of (1c) subtracted The dashed line has a slope of 0 79

linear range and read off the slope as 0.79. This gives a value for the dimension as $D_0 \approx 0.395$ which has to be compared with the value $D_0 = 0.39$ which we obtained from analysing the classical deflection function.

Next, let us consider the cross section as a function of the energy for fixed θ_0 ($\neq \theta_{R_j}$) and apply an analogous procedure. We expand $S_j(E)$ linearly around some E_0:

$$S_j(E) = S_j(E_0) + (E - E_0)T_j \tag{11}$$

where $T_j = \partial S_j / \partial E(E_0)$ is the time delay of trajectory Γ_j. The cross section becomes

$$\frac{d\sigma}{d\theta}(\alpha_0, E, \theta_0) = \sum_j c_j + \sum_{k<j} 2\sqrt{c_k c_j}\cos(\psi_{kj} - E(T_k - T_j)/\hbar) \tag{12}$$

with the ψ_{kj}s as constants. The pattern of delay time differences again reflects the fractal structure of the classical repeller [21]. Therefore, we take the Fourier transform $g(\Delta)$ of the cross section over an appropriate interval of energy values (α_0, θ_0 fixed), divide the frequency (delay time differences) axis into boxes, and count the number $Z(S)$ of boxes whose content is above the threshold S. Because in (12) the same weight factors c_j appear as in (7), we expect the same scaling behaviour (9) and (10) to hold.

From the treatment of the energy dependent cross section, more precisely from $g(\Delta)$, we can obtain an *additional* information. The probability density for finding a classical trajectory with time delay T is given by

$$P(T) = \kappa\, e^{-\kappa T} \tag{13}$$

in the limit of sufficiently large values of T. Here κ is the escape rate of the repeller. Correspondingly, the distribution of time delay differences must also show the same exponential behaviour. From a logarithmic plot of the Fourier transform of the cross section we can, therefore, read off κ as the slope of the *envelope*.

To give a numerical example for system (1), we choose $E \in [0.6, 0.602]$, $\alpha_0 = \pi$, $\theta_0 = 5.4$, $\hbar = 10^{-6}$. Figure 5 shows the logarithm of $g(\Delta)$. Inserted is a straight line of slope -0.4 which is a good fit to the envelope towards large time delay differences. The exact value of the escape rate is $\kappa = 0.42$ which comes out of an evaluation of the discontinuities in the deflection function. Next, we divide the time axis in figure 5 into 8192 boxes and count the number $Z(S)$ of boxes with contents above the variable

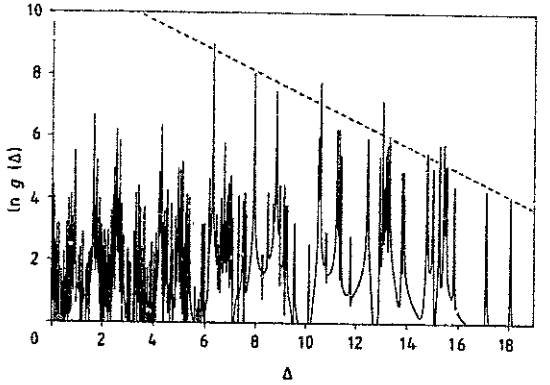

Figure 5. Logarithm of $g(\Delta)$, of the Fourier transform of the semiclassical differential cross section (computed in [21]) as a function of energy for $\theta = 5.4$, $\alpha = \pi$. The dashed line shows the envelope and yields an approximate value for the escape rate as $\kappa \approx 0.4$.

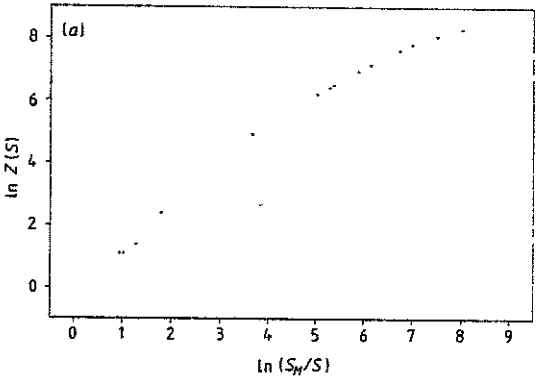

Figure 6(*a*). Logarithm of the number of boxes in the histogram of $g(\Delta)$ (see figure 5), whose content is larger than S against the logarithm of S_M/S ($S_M = 5000$)

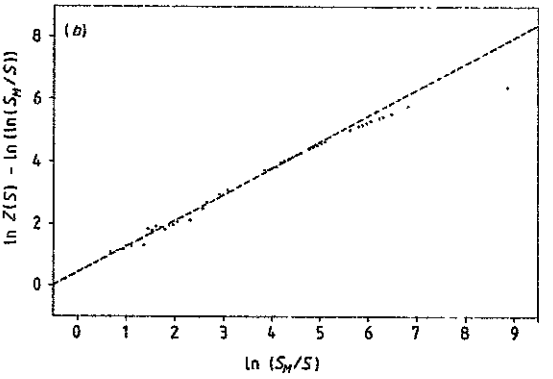

Figure 6(*b*). As figure 6(*a*), but with the logarithmic correction of (10) subtracted. The dashed line has a slope of 0.83.

threshold S. Figure 6 shows the plot of $\ln Z(S)$ with and without logarithmic corrections. Towards the right boundary of the plots a saturation occurs because of the finite number of boxes. Therefore, we read off the slope from the first part of the curve $\ln Z - \ln(\ln(S_M/S))$ and obtain a value of approximately 0.83.

It is worth mentioning that the knowledge of the escape rate and partial fractal dimension makes an accurate estimation of the Lyapunov exponent possible. Let us recall a famous relation valid for hyperbolic repellers in three variable flows [24]:

$$\lambda = \frac{\kappa}{1 - D_1} \tag{14}$$

where D_1 and λ are the partial information dimension and Lyapunov exponent, respectively, belonging to the natural measure on the repeller. The partial fractal dimension D_0 we deduced from the cross section data differs from $D_1 < D_0$, but the difference is typically rather small. (In our example at $E = 0.6$, e.g. $D_0 = D_1 + 0.01$.) Thus,

$$\lambda \approx \frac{\kappa}{1 - D_0} \tag{15}$$

is expected to be a good approximation of (actually an upper bound to) the Lyapunov exponent. Using the values $\kappa \approx 0.4$, $D_0 = 0.38$ we obtain $\lambda \approx 0.66$ which is close to the exact exponent $\lambda = 0.68$. Note that the approximate value is lower than the exact one due to our underestimation of the escape rate which happens to have an effect stronger than replacing D_1 by D_0.

Finally, we note that κ as obtained from $g(\Delta)$ yields the escape rate measured in *real* time. From the investigation of the deflection function one obtains, however, the escape rate κ_{map} on an appropriate Poincaré section, i.e. in *discrete* time. These two quantities are simply related via $\kappa_{\text{map}} = \kappa/\tau$ where τ is the averaged turnover time between two points of the repeller on the Poincaré section. Similarly, the Lyapunov exponent λ_{map} measured in discrete time is obtained as $\lambda_{\text{map}} = \lambda/\tau$ where τ is the *same* turnover time as above. As a consequence, (15) holds for the map in the form of $\lambda_{\text{map}} \approx \kappa_{\text{map}}/(1 - D_0)$. In our example $\tau \approx 2.46$.

4. Final remarks

This paper shows how characteristics of the classical strange repeller can be extracted out of the differential scattering cross section which is a clearly measurable quantity both classically and quantum mechanically. In the classical case, the fractal dimension can be read off from the pattern of rainbow singularities. Although we believe that the cross section contains more information, we have not succeeded in finding a practical method for deducing the escape rate from the classical data.

It is remarkable that both quantities can be obtained from the semiclassical cross section. The procedure relies essentially on the interference oscillations which are typical quantum effects. In contrast to the classical method, here we have to restrict our attention to a θ range which is away from rainbow singularities. This indicates that in the averaging out of the interference oscillations, which occurs in the transition from the quantum to the classical cross section, valuable information is discarded: the fractal dimension cannot be extracted out of a short θ interval classically but can be extracted semiclassically.

Our method requires two conditions to be fulfilled: first, it only works in the limit of small $\hbar$. In practical examples this means, that the wavelength of the incoming projectile is very small compared with the size of the target potential. Second, we have assumed that the incoming direction of the projectiles relative to the target is kept fixed. For real scattering experiments this usually requires that the orientation of the target is fixed in space. Otherwise, all interference oscillations are averaged out. Usually, these conditions are not fulfilled in the scattering of two microscopic particles off each other. However, they are fulfilled in the scattering of a particle off a macroscopic target, e.g. the scattering of an electron off electrically charged metallic objects. They are also fulfilled for the motion of ballistic electrons in mesoscopic semiconductors. In this case the motion is essentially two-dimensional and, therefore, it comes even closer to the case considered in this paper. Interestingly, the chaotic fluctuations of the conductivity of small semiconductors have recently been interpreted in terms of chaotic scattering [25].

Let us close with a remark on the relation of our results to the ones presented in [17]. There the energy correlation function of the scattering amplitude has been evaluated. This correlation contains an averaging process over small energy intervals. Thereby, the knowledge about the detailed fractal structure of chaos is lost. Consequently, as an essential measure of the classical repeller only the escape rate κ can be read off. In the method presented here we also obtain κ when disregarding the details of $g(\Delta)$ and looking at the asymptotic slope of the envelope only. This parallels exactly the extraction of κ as in [17]. By an evaluation of the fine fractal details of the Fourier spectrum, however, we obtain *in addition* the value of the partial fractal dimension D_0, information which is lost during any kind of averaging process.

Acknowledgments

The authors would like to thank G Eilenberger for the kind hospitality at the IFF of the KFA Jülich. One of us (TT) is indebted to A Bringer and T Vicsek for useful discussions.

Appendix. Derivation of equation (9)

When calculating the classical cross section, the incoming momentum is kept fixed and the impact parameter axis is covered evenly by projectiles. The deflection function $\theta(b)$ gives the scattering angle θ for the impact parameter b. All trajectories which go into the measured final direction contribute to the cross section $d\sigma/d\theta(\theta_0)$, i.e. all trajectories Γ_j which start with an impact parameter b_j such that $\theta(b_j)=\theta_0$. Their contribution to the cross section is c_j, as given by (2) taken at $b=b_j$. In the case of scattering chaos, the impact parameter axis is cut into an infinity of intervals I_k where the deflection function is continuous. Between these intervals a Cantor set of discontinuities remains.

Let the length of interval I_k be denoted by r_k. Using a resolution ε in measuring the impact parameter, the number $M(\varepsilon)$ of intervals resolved (i.e. the number of intervals I_k with $r_k > \varepsilon$) increases with decreasing ε. The gaps between the resolved intervals are of order ε and provide a coverage of the Cantor set of discontinuities. Its dimension D_0 was shown to agree with the partial fractal dimension of the chaotic

repeller [13]. The number of gaps is, however, practically $M(\varepsilon)$, therefore, one expects

$$M(\varepsilon) \approx \varepsilon^{-D_0}. \tag{A1}$$

The next important observation is that the deflection function looks similar in all intervals I_k, it is just scaled by the length r_k (for some figures see [18]). If there is a contribution c_j to the cross section from a trajectory Γ_j starting from interval I_j, then there are other trajectories Γ_k starting from all other intervals I_k and give contribution c_k to the cross section, where

$$c_k \approx \frac{r_k}{r_j} c_j \tag{A2}$$

in the limit of small intervals. Accordingly, if a threshold S is prescribed, the number $\bar{N}(S)$ of c_k values with $c_k > S$ increases with the same power D_0 which gives the growth of the number of intervals in (A1).

$$\bar{N}(S) \approx \left(\frac{S_M}{S}\right)^{D_0} \tag{A3}$$

where S_M is some constant, essentially the maximum of c_k. For simplicity, let us assume for the moment that $S_M = 1$, or that S is measured in units of S_M. Note that in the semiclassical sum (4) not the c_js but rather their square roots appear. Taking the square root of the weights in (A3) is equivalent to taking the square of the threshold S or to taking twice the exponent. Therefore, the number $N(S)$ of values $\sqrt{c_j}$ which lie above S is given by

$$N(S) \approx S^{-2D_0} \tag{A4}$$

and the density $n(S)$ of contributions around the value S is

$$n(S) = -\frac{\mathrm{d}N}{\mathrm{d}S} \approx 2D_0 S^{-2D_0-1}. \tag{A5}$$

For the cross section in (7), (8) or (12) we need the number of cross terms for which $\sqrt{c_k c_j} > S$. This inequality can be fulfilled for any k with $\sqrt{c_k} = a$, if j is chosen such that $\sqrt{c_j} > S/a$. The density $n(a)$ of contributions with $\sqrt{c_k} = a$ is given according to (A5) by $n(a) \approx 2D_0 a^{-2D_0-1}$. The number $N(S/a)$ of contributions with $\sqrt{c_j} > S/a$ is obtained from (A4) as

$$N(S/a) \approx S^{-2D_0} a^{2D_0}.$$

The number $Z(S)$ of all pairs with $\sqrt{c_k c_j} > S$ can then be found by multiplying $n(a)$ with $N(S/a)$ and integrating over all allowed values of a. The upper limit of a is 1 (or S_M in the unscaled case). For a smaller than S, the value of S/a in the argument of N would be larger than 1, which is not allowed. In order to avoid double counting of all contributions, we take as lower limit of a the value $\sqrt{S}$. Thus, one finds

$$Z(S) = \int_{\sqrt{S}}^{1} n(a) N(S/a)\, \mathrm{d}a = D_0 (S)^{-2D_0} \ln(1/S). \tag{A6}$$

After replacing $1/S$ by S_M/S we obtain (9).

References

[1] Eckhardt B 1988 *Physica* **33D** 89
[2] Smilansky U 1990 *Chaos and Quantum Physics* ed M-J Giannoni *et al* (New York: Elsevier)
[3] Blümel R 1991 *Directions in Chaos* vol 4, ed Bai-lin Hao *et al* (Singapore: World Scientific), in press
[4] Tél T 1990 *Directions in Chaos* vol 3, ed Bai-lin Hao (Singapore: World Scientific) pp 149–221
[5] Eckhardt B and Jung C 1986 *J. Phys. A Math. Gen* **19** L829
Jung C and Scholz H J 1987 *J. Phys. A: Math. Gen.* **20** 3607
[6] Eckhardt B 1987 *J Phys A: Math. Gen.* **20** 5971
[7] Hénon M 1988 *Physica* **33D** 132
[8] Troll G and Smilansky U 1989 *Physica* **35D** 34
[9] Gaspard P and Rice S A 1989 *J. Chem. Phys* **90** 2225, 2242, 2255
[10] Tél T 1989 *J. Phys A: Math. Gen.* **22** L691
[11] Cvitanović P and Eckhardt B 1989 *Phys Rev. Lett.* **63** 823
[12] Bleher S, Ott E and Grebogi C 1989 *Phys. Rev. Lett.* **63** 919
Bleher S, Grebogi C and Ott E 1990 *Physica* **46D** 87
[13] Kovács Z and Tél T 1990 *Phys Rev Lett* **64** 1617
[14] Jung C and Richter P 1990 *J Phys. A: Math. Gen* **23** 2847
[15] Chen Q, Ding M and Ott E 1990 *Phys Lett* **147A** 450
[16] Doron E, Smilansky U and Frenkel A 1990 *Phys. Rev. Lett.* **65** 3072; 1990 Chaotic scattering and transmission fluctuations *Preprint*
[17] Blumel R and Smilansky U 1988 *Phys. Rev Lett.* **60** 477; 1989 *Physica* **36D** 111; 1990 *Phys Rev Lett.* **64** 241
[18] Jung C and Pott S 1989 *J Phys A Math Gen* **22** 2925
[19] Grassberger P 1986 *Chaos* ed A V Holden (Manchester: Manchester University Press) p 261
[20] Tél T, Fülop A and Vicsek T 1989 *Physica* **159A** 155
Vicsek T, Family F and Meakin P 1990 *Europhys Lett* **12** 217
[21] Jung C and Pott S 1990 *J Phys. A. Math. Gen* **23** 3729
[22] Miller W H 1975 *Adv. Chem. Phys.* **30** 77
[23] Jung C 1990 *J. Phys A: Math. Gen.* **23** 1217
[24] Kantz H and Grassberger P 1985 *Physica* **17D** 75
[25] Roukes M L and Alerhand O L 1990 *Phys Rev. Lett.* **65** 1651
Jalabert R A, Baranger H U and Stone A D 1990 *Phys. Rev. Lett.* **65** 2442